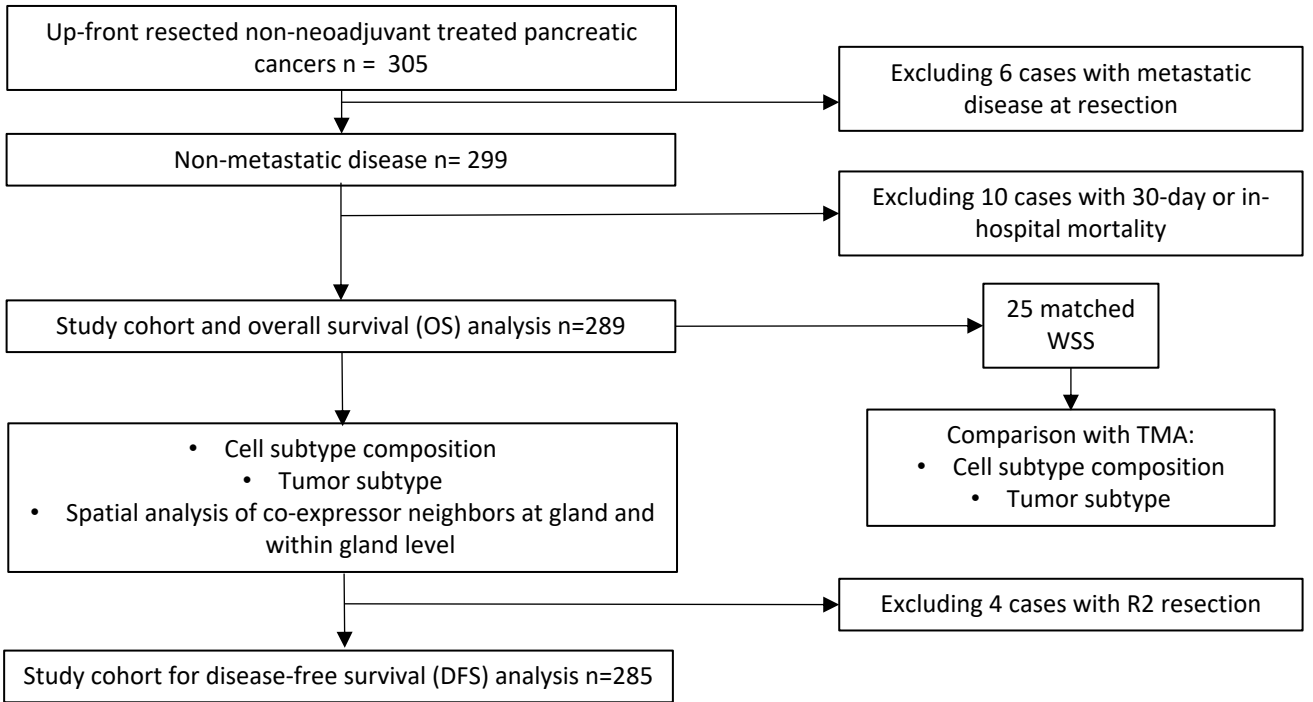
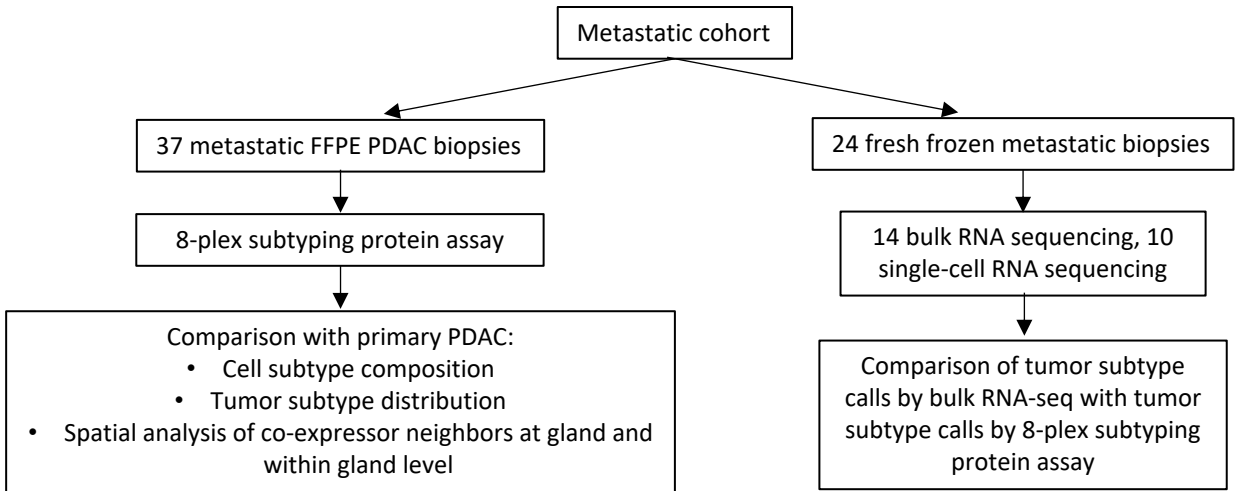


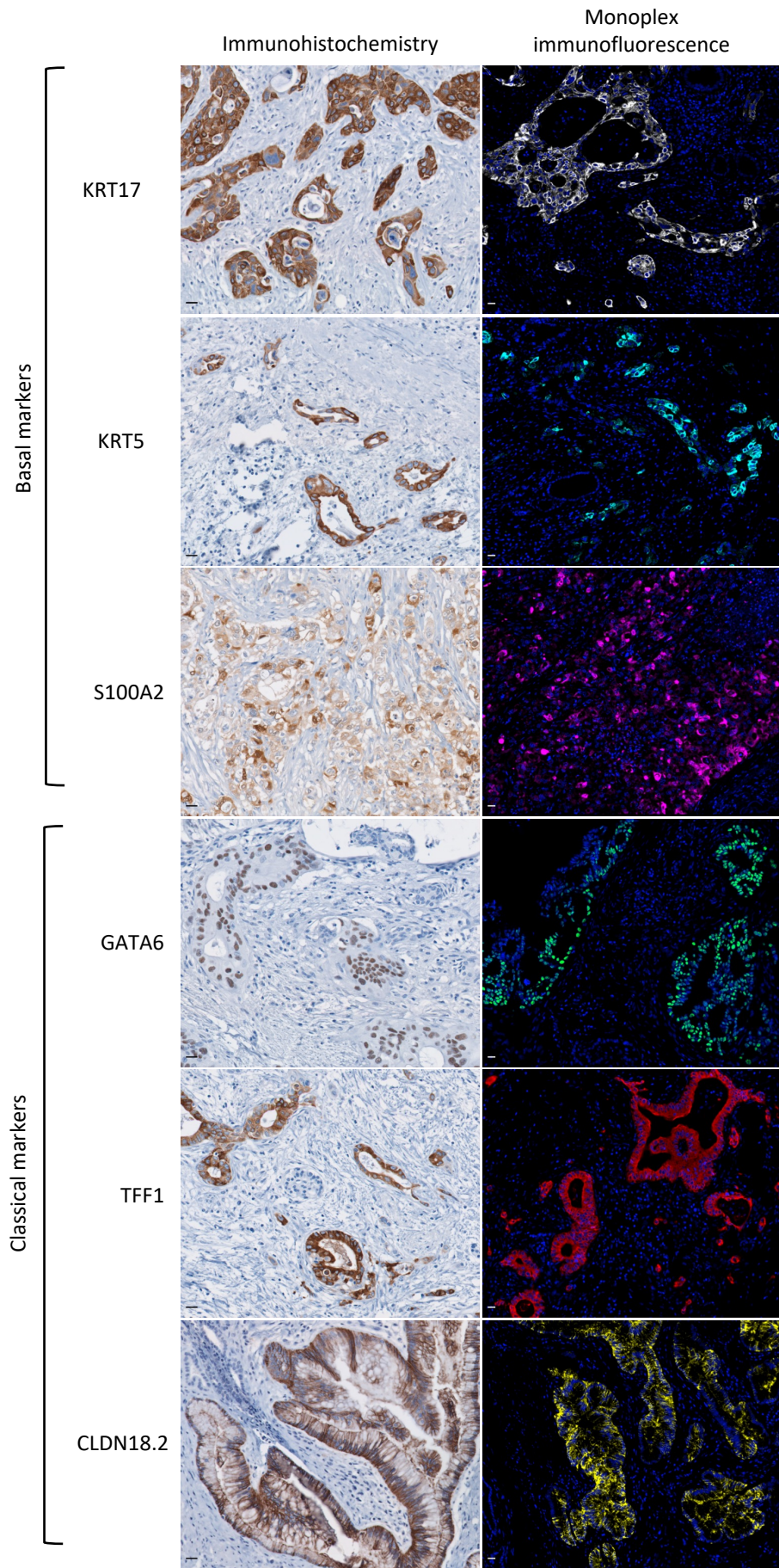
A.



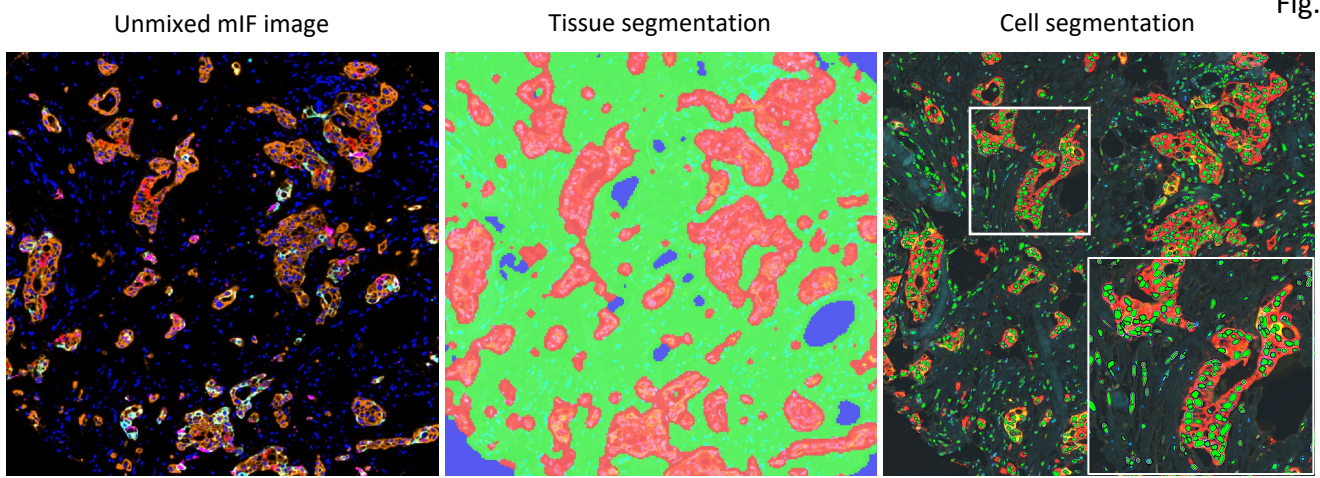
B.



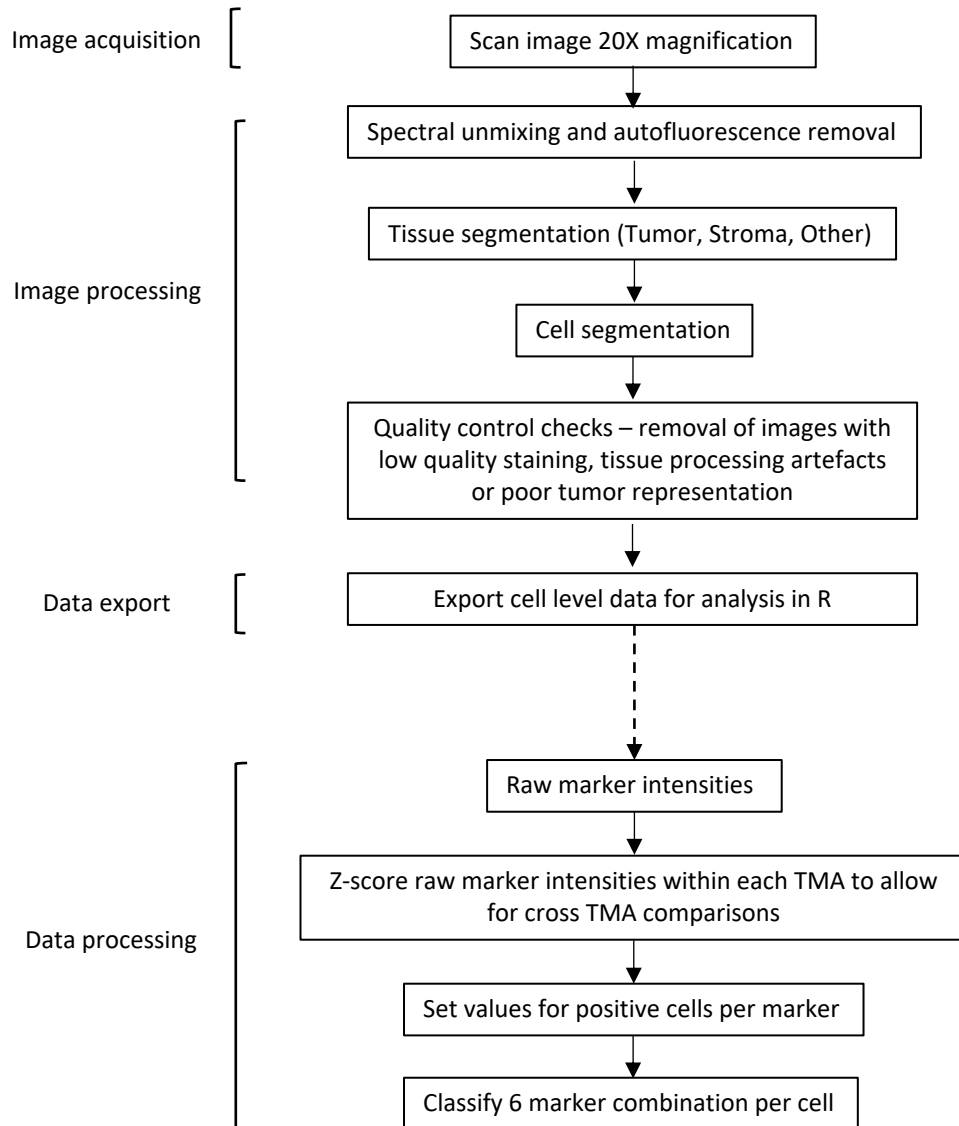
Supplementary figure S1. Study cohort summary. A: Primary resection cohort. 289 cases were included in the study cohort and overall survival analyses. DF/BWCC: Dana-Farber/Brigham and Women's Cancer Centre. URM: University of Rochester Medical Centre. SCI: Stanford Cancer Institute. B: Metastatic biopsy cohort. 37 cases were included in the study cohort and 24 matched fresh or frozen metastatic biopsies had RNA-sequencing data available (14 bulk-RNA sequencing, 10 single cell RNA-sequencing).



Supplementary figure S2. Single marker immunohistochemistry and monoplex immunofluorescence in primary PDAC specimens. Left panel, immunohistochemistry (top to bottom): KRT17, KRT5, S100A2, GATA6, TFF1, CLDN18.2. Right panel, monoplex immunofluorescence (top to bottom): KRT17 (Opal 520), KRT5 (Opal 480), S100A2 (Opal 650), GATA6 (Opal 540), TFF1 (Opal 690), CLDN18.2 (Opal 570).

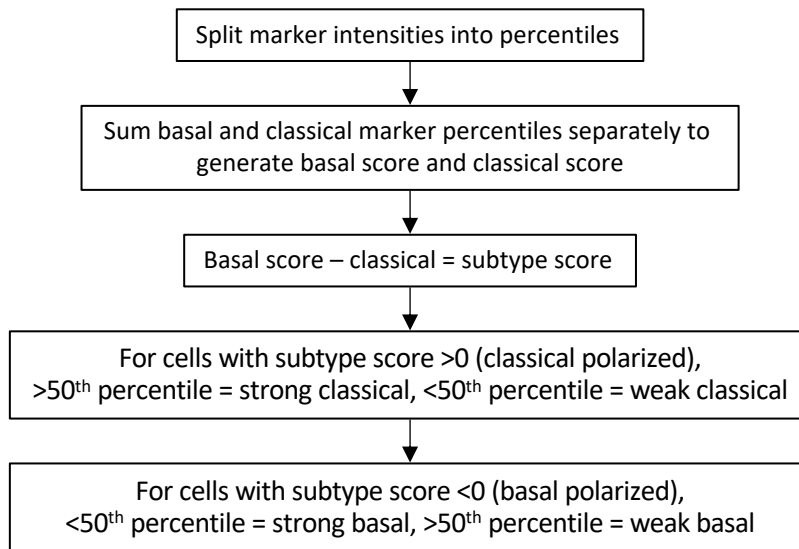


B.

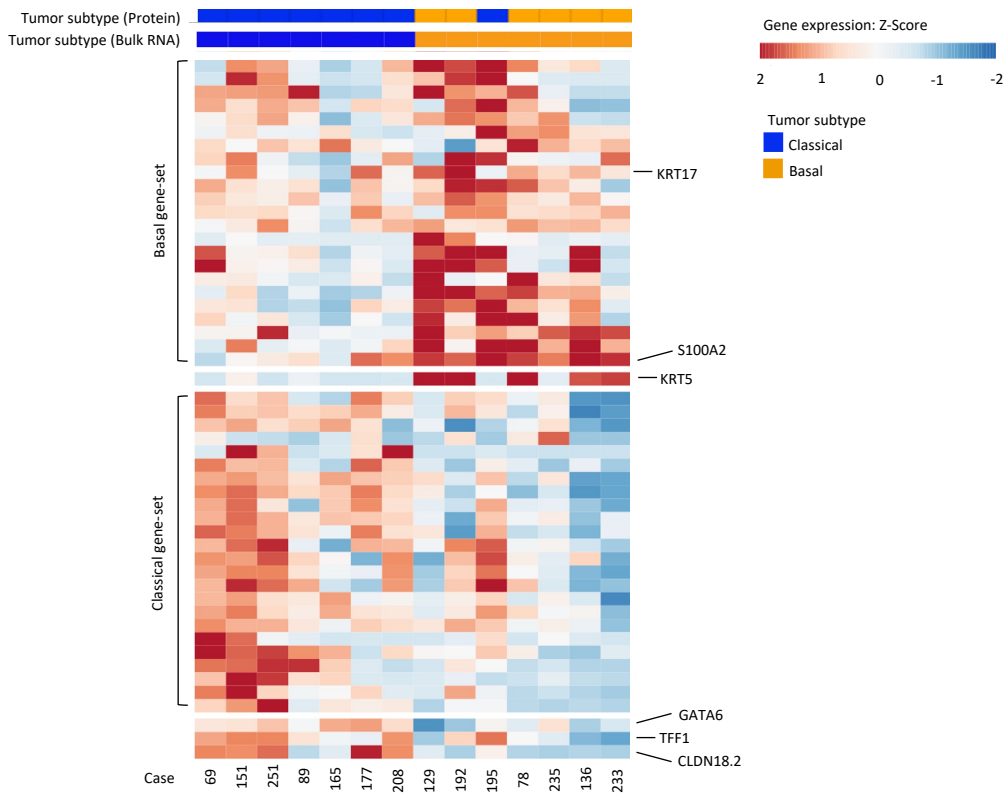


Supplementary figure S3. Image and data processing. A: (Left to right) Representative images of unmixed multiplex immunofluorescence image, tissue segmentation (red: tumor, green: stroma: blue: other/non-tissue) and cell segmentation (green: nuclei). B: Workflow for image processing and data analysis.

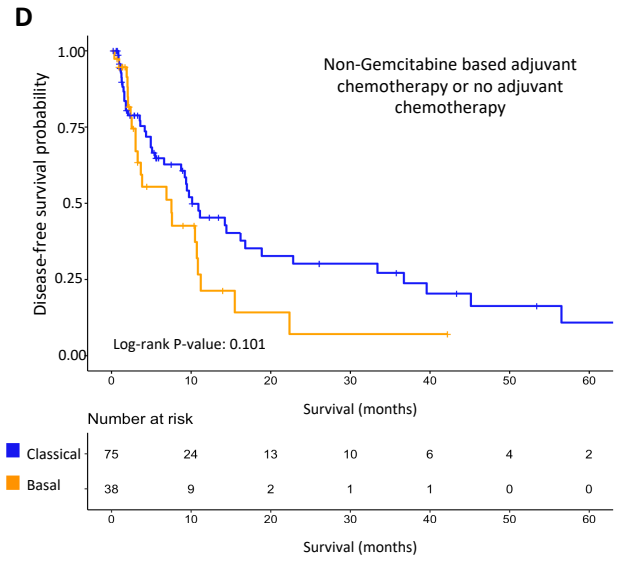
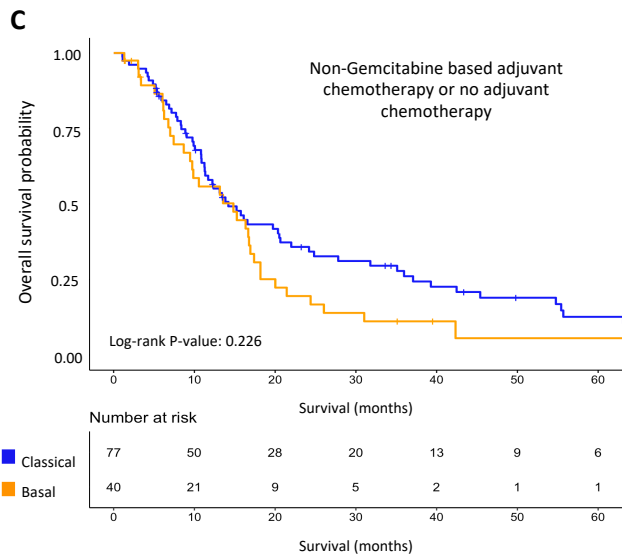
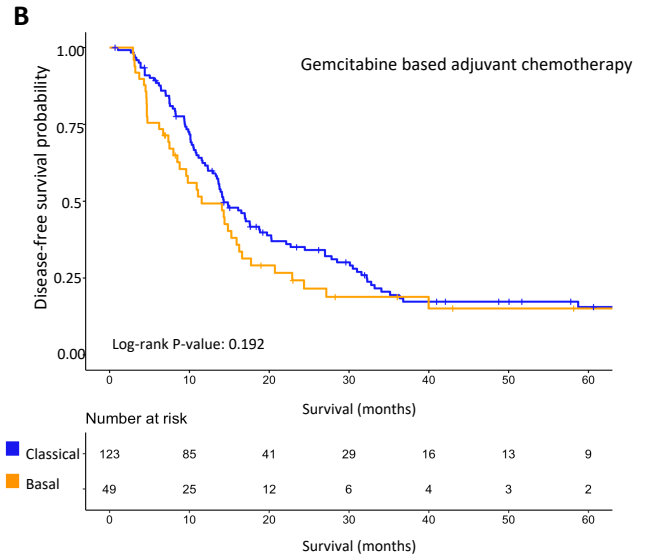
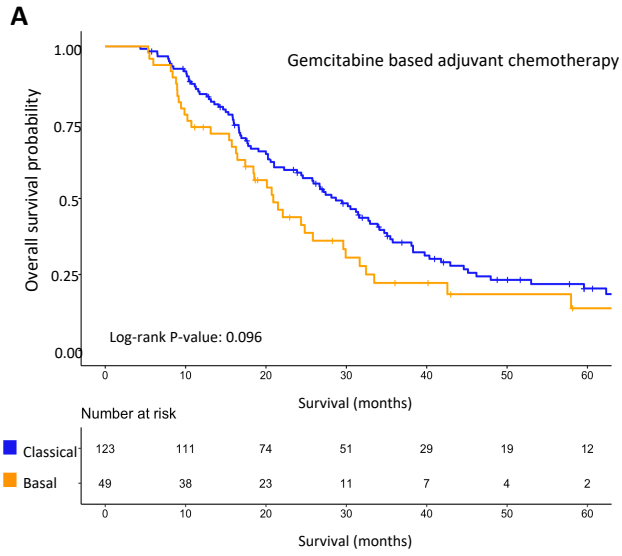
A.



Supplementary figure S4. Co-expressor cell polarization methodology. A: Data analysis workflow for co-expressor cell polarization.

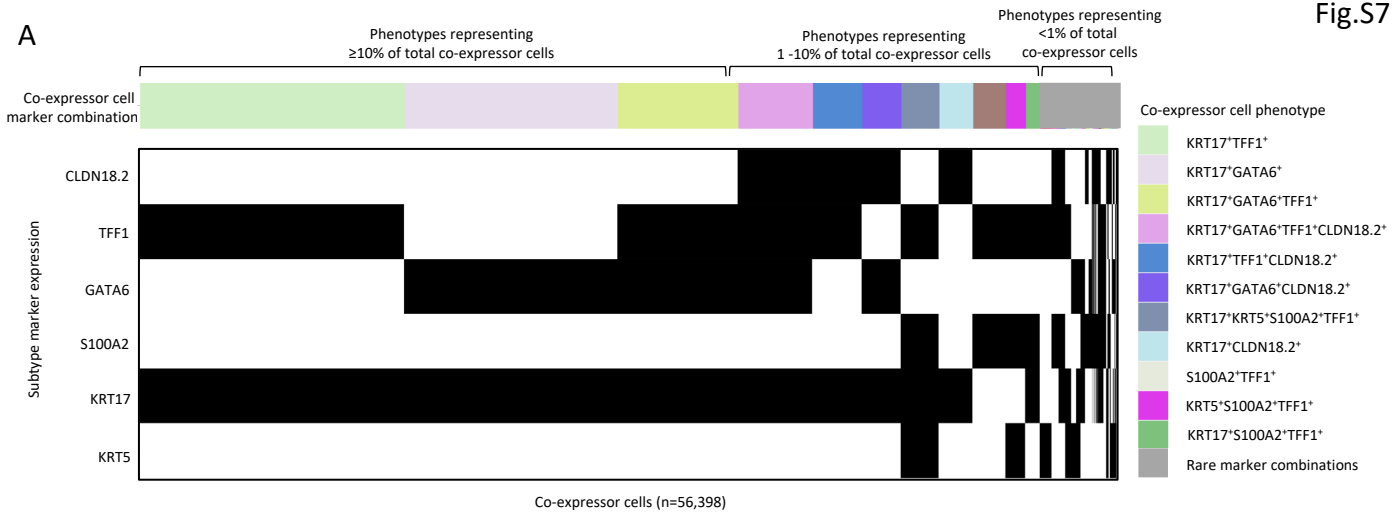


Supplementary figure S5. Orthogonal validation of multiplex immunofluorescence with RNA-sequencing. A: Comparison of multiplex immunofluorescence (mIF) and bulk RNA-sequencing of 14 metastatic biopsies. Top: Tumor subtype by multiplex immunofluorescence. Middle: Tumor subtype by bulk RNA-seq. Bottom: gene expression using bulk RNA-seq.



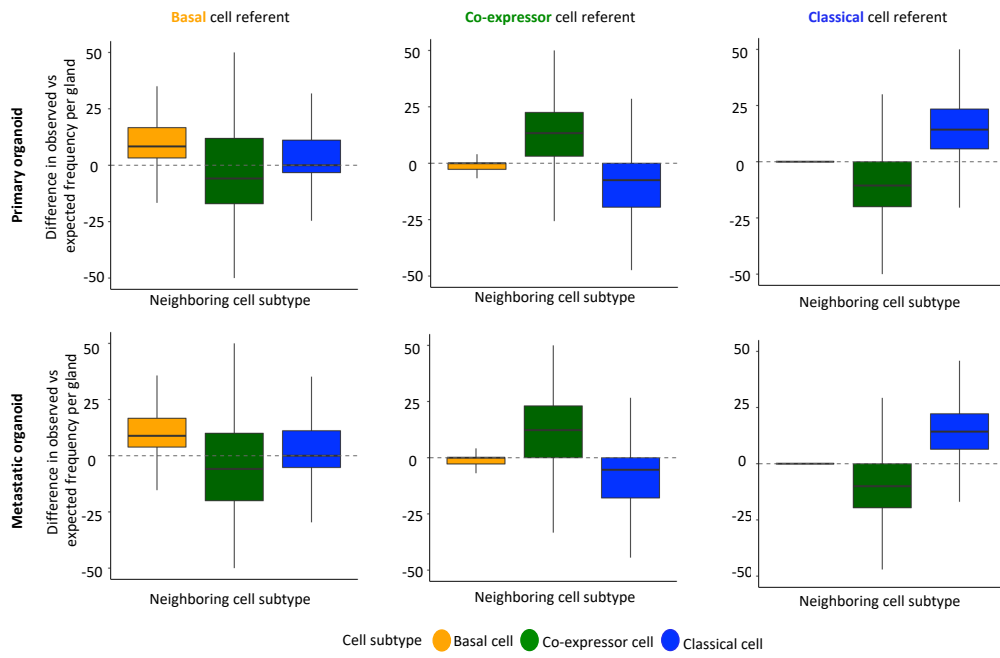
Supplementary figure S6. Kaplan-Meier curves for overall survival and disease-free survival by basal-classical expression subtype according to adjuvant treatment received. A: Association of tumor subtype with overall survival (OS) in patients treated with adjuvant gemcitabine or gemcitabine combination). B: Association of tumor subtype with disease-free survival (DFS) in patients treated with adjuvant gemcitabine or gemcitabine combination). C: Association of tumor subtype with OS in patients treated with non-gemcitabine based adjuvant chemotherapy or no adjuvant chemotherapy. D: Association of tumor subtype with DFS in patients treated with non-gemcitabine adjuvant chemotherapy or no chemotherapy. Log-rank p-values shown for comparison of survival among patients with basal and classical tumors.

A

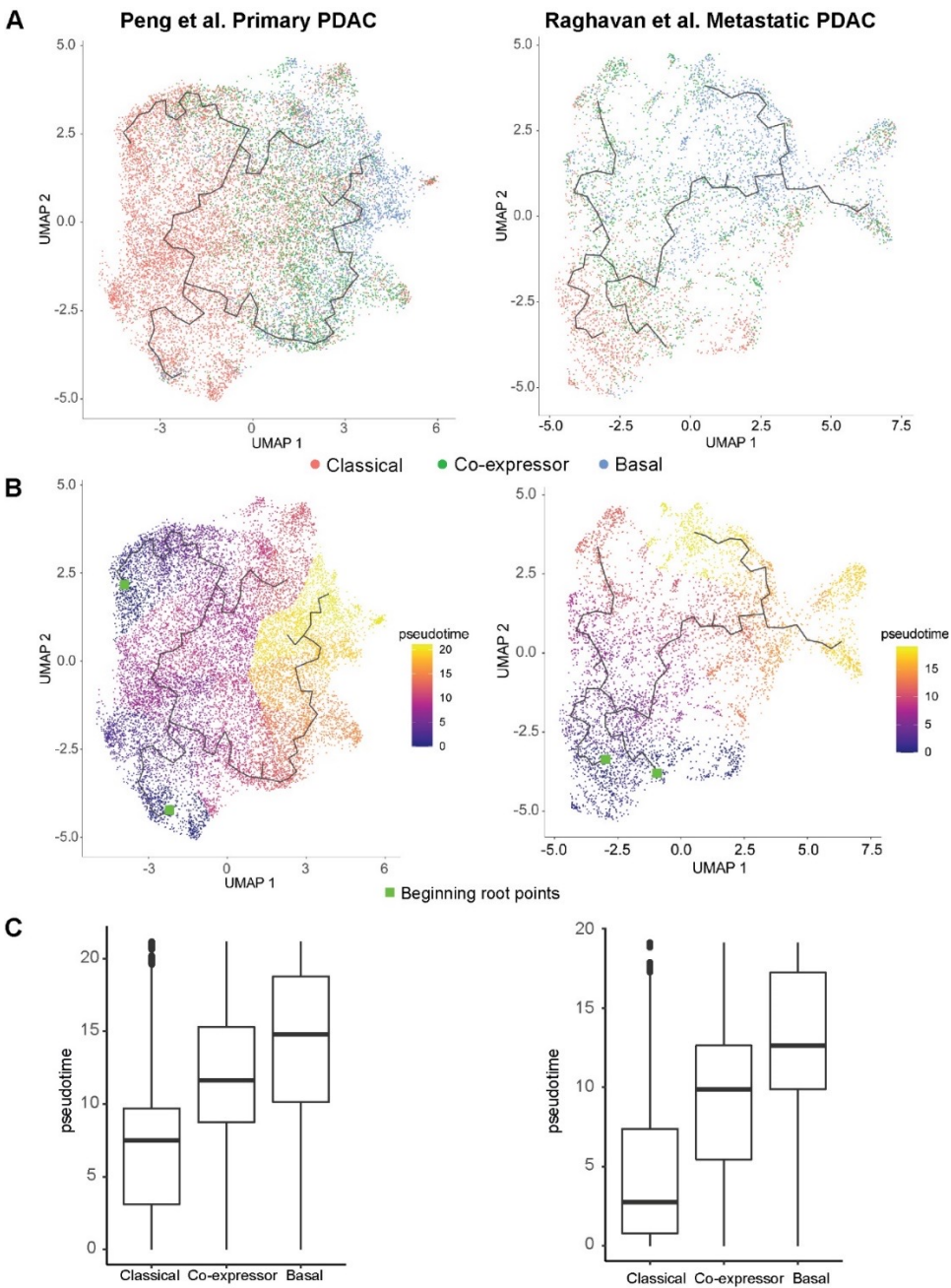


Supplementary figure S7. Co-expressor cell phenotype frequencies. The combinations KRT17⁺TFF1⁺, KRT17⁺GATA6⁺ and KRT17⁺GATA6⁺TFF1⁺ represented the three most common phenotypes for co-expressor cells (n=56,398) in our primary resection cohort.

A.



Supplementary figure S8. Direct neighbor analysis in patient-derived organoids. Direct neighbor analysis with comparison of expected and observed frequencies of subtypes by cell of reference and specimen type (primary and metastatic patient-derived organoids). Basal cells neighbor basal cells and classical cells neighbor classical cells more frequently than expected by chance. Difference between observed and expected frequencies per gland unit depicted (Mann-Whitney test between observed and expected frequencies).



Supplementary figure S9. Trajectory and Pseudotime Analysis of the Peng et al. and Raghavan et al. PDAC datasets. A. UMAP embedding of tumor cells from Peng et al. (left) and Raghavan et al. (right), showing the location of the classical, basal, and co-expressor cell types, overlaid with the predicted cell trajectory from Monocle3, as indicated by the black line. B. The same UMAP embeddings as in A, now colored with the pseudotime value of each cell, showing an increase in pseudotime as the cell trajectory moves from classical to basal cell types through co-expressor cell intermediates. Starting root points for the pseudotime analysis were chosen in the classical cell populations, as indicated by green square. C. Quantification of pseudotime values for each cell type indicated in B, showing that the co-expressor cells contain intermediate pseudotime values between the classical and basal transcriptional cell types in this analysis (all p-values <0.0001 for Kruskal-Wallis test and pairwise comparisons using Wilcoxon rank sum test).